

Sulfur K-Edge EXAFS Studies of Cadmium-, Zinc-, Copper-, and Silver-Rabbit Liver Metallothioneins

Ziqi Gui, Anna Rae Green, Masoud Kasrai, G. Michael Bancroft, and Martin J. Stillman*

Department of Chemistry, The University of Western Ontario, London, Ontario, Canada N6A 5B7

Received December 19, 1995[⊗]

The structures of metal–thiolate clusters in Zn₇-MT, Cd₇-MT, Cu₁₂-MT, Ag₁₂-MT, and Ag₁₇-MT from rabbit liver have been investigated by sulfur K-edge X-ray absorption spectroscopy (XAS). In addition to providing metal–cysteinyl sulfur bond lengths, the sulfur K-edge EXAFS data provide the first direct evidence for mixtures of bridging and terminal sulfurs in Cu-MT and Ag-MT. The Zn–S and Cd–S bond lengths for tetrahedrally coordinated Zn₄(SPh)₁₀²⁻ and Cd₄(SPh)₁₀²⁻ compounds obtained from sulfur K-edge EXAFS data are 2.35 ± 0.03 and 2.52 ± 0.02 Å, respectively. Zn–S and Cd–S bond distances of 2.34 ± 0.03 Å for Zn₇-MT and 2.54 ± 0.02 Å for Cd₇-MT, respectively, calculated from sulfur K-edge EXAFS measurements, are consistent with the previously reported results from metal K-edge EXAFS data. Analysis of the sulfur K-edge EXAFS data for Cu₁₂-MT indicates that Cu(I) is trigonally coordinated to sulfurs at a distance of 2.25 ± 0.01 Å. Significant changes in CD spectra observed between Ag₁₂-MT 1 and Ag₁₇-MT 1 indicate that the modification of the three-dimensional structure occurs when Ag₁₇-MT 1 is formed from Ag₁₂-MT 1 as Ag(I) is added to the Ag₁₂-MT 1. The Ag–S bond distances of 2.45 ± 0.02 and 2.44 ± 0.03 Å in Ag₁₂-MT 1 and Ag₁₇-MT 1, respectively, calculated from the sulfur K-edge EXAFS measurements, lead us to conclude that the Ag(I) in both Ag₁₂-MT 1 and Ag₁₇-MT 1 is digonally coordinated by thiolates. The number of metals bonded to sulfur in both model compounds and metal-containing metallothioneins is estimated from sulfur K-edge EXAFS measurements to be in the range 1.2–1.7, depending on the fraction of bridging sulfurs present in compounds. Unlike the spectral data recorded during Cu(I) binding, where sharp changes take place past 12 Cu(I), the CD data for Ag-MT 1 show little variation over the entire range of Ag(I):MT molar ratios. This result, established by both low- and high-energy optical methods, suggests that the three-dimensional structure of the metal-binding sites in metallothioneins is strongly influenced by the fraction of bridging sulfur. This analysis is the first to provide direct support for the presence of a clustered Ag–S structure for the Ag₁₇-MT 1 species. These data also suggest that the structures in Ag(I) and Cu(I) metallothioneins are probably quite different.

Introduction

Mammalian metallothioneins (MT) are a class of low molecular weight, cysteine-rich proteins.¹ Rabbit liver metallothionein contains 20 cysteines out of a total of 61 or 62 amino acids with a complete absence of aromatic residues and histidine and a relatively large amount of serine and lysine,^{1b} as shown in Figure 1. MT binds many metal ions, especially those with the d¹⁰ configuration, such as Zn(II), Cd(II), Cu(I), Ag(I), and Hg(II), with high affinity.^{1a,c,d} Metallothioneins are believed to play a general role in the metabolism of the essential metals^{2a} and in the detoxification of nonessential metals^{2b} on the basis of the observation that, following exposure of animals to cadmium, zinc, copper, mercury, and other metals, not only does the isolated protein contain these metals, but the total metallothionein level in the tissues is markedly increased as well.

A number of structural studies have provided insight into the metal-binding sites in MT.¹ To date, the structures of Zn- and

Cd-containing metallothioneins have been described from analysis of NMR spectroscopy,^{3,4} X-ray crystallography,⁵ and optical spectroscopies.⁶ On the basis of these results, it has been shown that mammalian metallothioneins bind metals in two domains: an α domain with an M₄S₁₁ cluster and a β domain with an M₃S₉ cluster.^{3–5} Zn(II) and Cd(II) are exclusively tetrahedrally coordinated to cysteinyl thiolates in both domains. Figure 2 shows a representation of the two-domain structure for M₇-MT (M = Cd, Zn). Despite the wide range of metals that bind to metallothionein, these structures are still under investigation, because structures involving metals other than Cd(II) and Zn(II) are much more difficult to determine.

* To whom correspondence should be addressed. Tel: (519) 661-3821. Fax: (519) 661-3022. Internet: Stillman@uwo.ca.

[⊗] Abstract published in *Advance ACS Abstracts*, September 1, 1996.

- (1) (a) *Metallothionein II*; Kagi, J. H. R., Kojima, Y., Eds.; Birkhauser Verlag: Basel, 1987. (b) *Metallothionein III*; Suzuki, K. T., Imura, N., Kimura, M., Eds.; Birkhauser Verlag: Basel, 1993. (c) *Metallothioneins. Synthesis, structure and properties of metallothioneins, phytochelatins and metal-thiolate complexes*; Stillman, M. J., Shaw, C. F., III, Suzuki, K. T., Eds.; VCH Publishers: New York, 1992. (d) Kagi, J. H. R. In *Metallothionein III*; Suzuki, K. T., Imura, N., Kimura, M., Eds.; Birkhauser Verlag: Basel, 1993; pp 29–56. (e) Stillman, M. J. *Coord. Chem. Rev.* **1995**, *144*, 461–511.
- (2) (a) Bremner, I. *Experientia, Suppl.* **1987**, *52*, 81–107. (b) Webb, M. *Experientia, Suppl.* **1987**, *52*, 109–134.

- (3) (a) Otvos, J. D.; Armitage, I. M. *Proc. Natl. Acad. Sci. U.S.A.* **1980**, *77*, 7094–7098. (b) Neuhauser, D.; Wagner, G.; Vasak, M.; Kagi, J. H. R.; Wuthrich, K. *Eur. J. Biochem.* **1985**, *151*, 257–273.
- (4) (a) Frey, M. H.; Wagner, G.; Vasak, M.; Sorensen, O. W.; Neuhaus, D.; Worgotter, E.; Kagi, J. H. R.; Ernst, R. R.; Wuthrich, K. *J. Am. Chem. Soc.* **1985**, *107*, 6847–6851. (b) Arseniev, A.; Schultze, P.; Worgotter, E.; Braun, E.; Wagner, G.; Vasak, M.; Kagi, J. H. R.; Wuthrich, K. *J. Mol. Biol.* **1988**, *201*, 637–657. (c) Messerle, B. A.; Schaffer, A.; Vasak, M.; Kagi, J. H. R.; Wuthrich, K. *J. Mol. Biol.* **1992**, *225*, 433–443.
- (5) (a) Robbins, A. H.; McRee, D. E.; Williamson, M.; Collett, S. A.; Xuong, N. H.; Furey, W. F.; Wang, B. C.; Stout, C. D. *J. Mol. Biol.* **1991**, *221*, 1269–1293. (b) Robbins, A. H.; Stout, C. D. In *Metallothioneins*; Stillman, M. J., Shaw, C. F., III, Suzuki, K. T., Eds.; VCH: New York, 1992; Chapter 3, pp 31–54.
- (6) (a) Stillman, M. J.; Cai, W.; Zelazowski, A. J. *J. Biol. Chem.* **1987**, *262*, 4538–4558. (b) Stillman, M. J.; Zelazowski, A. J. *J. Biol. Chem.* **1988**, *263*, 6128–6133. (c) Stillman, M. J. In *Metallothioneins*; Stillman, M. J., Shaw, C. F., III, Suzuki, K. T., Eds.; VCH: New York, 1992; Chapter 4, pp 55–127.

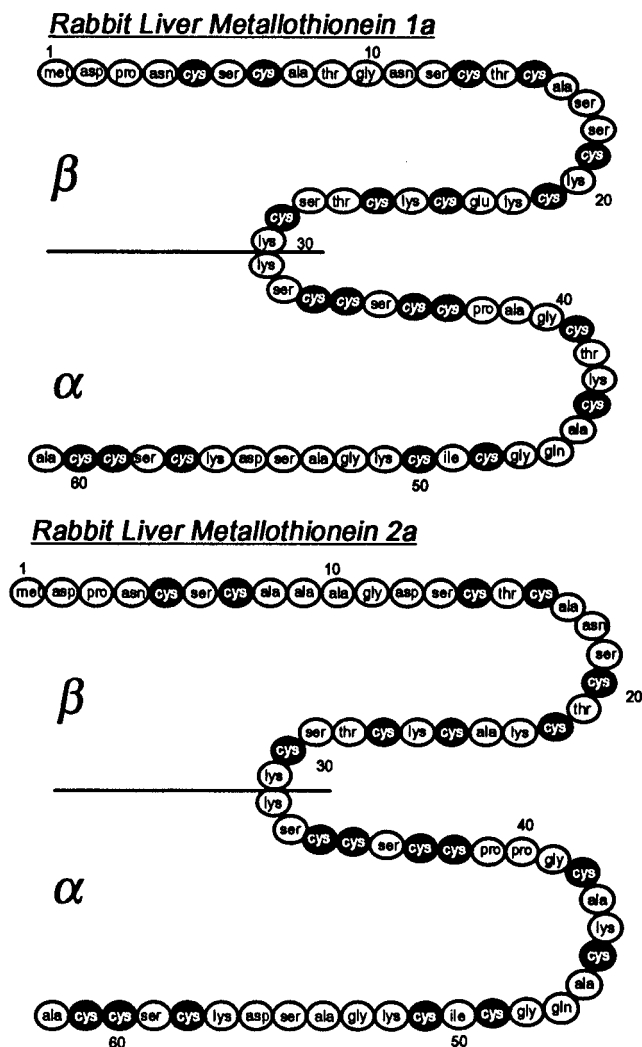


Figure 1. Sequences for rabbit liver metallothioneins 1a, and 2a, based on ref 1c. The dark ovals represent cysteine residues.

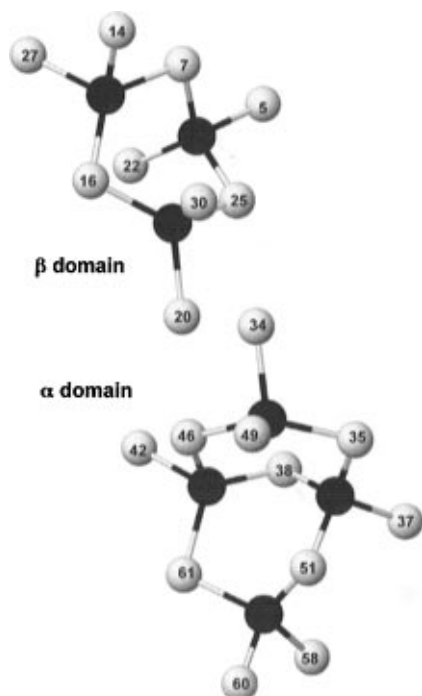


Figure 2. The two-domain structure for Cd₇-MT 2. The numbers refer to the amino acid position in the sequence taken from refs 3a and 5b.

Extended X-ray absorption fine structure (EXAFS) spectroscopy has been intensively used to study the structure of various

metal-containing metallothioneins. Garner *et al.*^{7,8} and, very recently, Jiang *et al.*⁹ reported results from Zn K-edge EXAFS measurements for Zn₇-MT, where average Zn–S bond distances have been determined to be 2.29 Å for the sheep liver metallothionein⁷ and 2.33–2.35 Å^{8,9} for the rabbit liver metallothionein with the coordination number of zinc 4. Abrahams *et al.*¹⁰ have published the results of a Cd K-edge EXAFS study of Cd₅Zn₂-MT and Cd₇-MT from rat liver. They detected no significant difference between the EXAFS data associated with the Cd K-edges of Cd₅Zn₂-MT and Cd₇-MT 1. Analysis of Cd K-edge EXAFS measurements carried out by Jiang *et al.*⁹ concluded that each cadmium is coordinated to four cysteinyl sulfurs with an average Cd–S bond distance 2.50 Å. The results from the Zn and Cd K-edge EXAFS spectra of the Zn- and the Cd-MT are consistent with the proposed structure that each zinc or cadmium atom has an environment consisting of a single shell of four sulfur atoms at 2.33–2.35 Å for Zn₇-MT and 2.50–2.53 Å for Cd₇-MT.

Smith *et al.*¹¹ reported both Cu K-edge XANES and EXAFS spectra from the low molecular weight Cu-MT from *Neurospora crassa*. They concluded that the X-ray absorption edge and the EXAFS data of Cu-MT were most consistent with three- or four-coordinate geometry around the Cu, with an average Cu environment of three or four sulfur atoms at 2.20 Å, and excluded the previously proposed two-coordinate linear-chain structure.¹² A Cu K-edge X-ray absorption study of the Cu₆-β MT from rat liver has been reported by George and co-workers.¹³ They proposed a trigonal bipyramid for the Cu₆S₉ cluster in which Cu occupies each vertex and a cysteinyl sulfur bridges each of the nine edges. The average Cu–S distance was calculated to be 2.25 Å. Studies on Cu K-edge X-ray absorption spectroscopy of cuprous–thiolate clusters in proteins and model systems have been reported by Pickering *et al.*¹⁴ In their study, a correlation was made between the Cu–S bond lengths and a proposed fraction of digonal and trigonal copper sites in different copper(I)-containing metallothioneins based on Cu K-edge EXAFS curve-fitting analysis. These authors claimed that in rat liver Cu₆-β MT 30% of the Cu(I) exists in digonal binding sites; this is in contrast to a previous report¹³ in which only trigonal geometry was proposed for copper(I) that was present with an average Cu–S bond length of 2.25 Å.

Lu *et al.*¹⁵ first reported S L-edge XANES spectra of group IIB metallothioneins. The results showed that the XANES spectrum of Hg₁₈-MT 2 was very different from the spectra of M₇-MT (M = Zn, Cd, Hg), which supported the previous suggestion¹⁶ that Hg₁₈-MT 2 adopts a completely different structure when compared with known M₇-MT species in terms of the sulfur environment. The Hg-MT structure has been further investigated using X-ray absorption fine structure spectroscopy by Jiang *et al.*⁹ For Hg₇-MT 2 the nearest-neighbor Hg–S bond length and coordination number have been determined to be 2.33 ± 0.02 Å and 2, respectively. In the

- (7) Garner, C. D. *J. Inorg. Biochem.* **1982**, *16*, 253–256.
- (8) Abrahams, I. L.; Bremner, I.; Deakun, G. P.; Garner, C. D.; Hasnain, S. S. *Biochem. J.* **1986**, *236*, 585–589.
- (9) Jiang, D. T.; Heald, S. M.; Sham, T. K.; Stillman, M. J. *J. Am. Chem. Soc.* **1994**, *116*, 11004–11013.
- (10) Abrahams, I. L.; Garner, C. D. *J. Am. Chem. Soc.* **1985**, *107*, 4596–4597.
- (11) Smith, T. A.; Lerch, K.; Hodgson, K. O. *Inorg. Chem.* **1986**, *25*, 4677–4680.
- (12) Furey, W. F.; Robbins, A. H.; Clancy, L. L.; Winge, D. R.; Wang, B. C.; Stout, C. D. *Science (Washington, D.C.)* **1986**, *231*, 704–710.
- (13) George, G. N.; Winge, D.; Stout, C. D.; Cramer, S. P. *J. Inorg. Biochem.* **1986**, *27*, 213–220.
- (14) Pickering, I. J.; George, G. N.; Dameron, C. T.; Kurz, D. B.; Winge, D. R.; Dance, I. G. *J. Am. Chem. Soc.* **1993**, *115*, 9498–9505.
- (15) Lu, W.; Kasrai, M.; Bancroft, G. M.; Stillman, M. J.; Tan, K. H. *Inorg. Chem.* **1990**, *29*, 2561–2563.
- (16) Cai, W.; Stillman, M. J. *J. Am. Chem. Soc.* **1988**, *110*, 7872–7873.

proposed new structure, each Hg(II) is coordinated to four cysteinyl sulfurs with two unusually short bonds and two unusually long bonds,⁹ which is different from the previously reported result for Hg₇-MT, where the coordination number was determined to be 3.¹⁷ For Hg₁₈-MT 2, the local structure has been shown to involve nearest-neighbor Hg-S bond lengths of 2.42 ± 0.03 Å with 2-fold sulfur coordination as well as a Hg-Cl shell at 2.57 ± 0.03 Å,⁹ which accounts for the strong dependence of Hg₁₈-MT 2 formation on the presence of chloride ions in the solution.¹⁸

Silver binding to metallothionein was first examined by Piotrowski's group¹⁹ as part of a survey of the capability of metals to induce synthesis of metallothionein in the liver and kidneys. Various values for the maximum number of Ag(I) that can bind MT have been reported. Scheuhammer and Cherian²⁰ used silver as a potential metal for the estimation of the concentration of metallothionein in tissue samples and in solutions. They found that saturation occurred at 17.3 Ag(I) rather than the anticipated 20 Ag(I) for 1:1 Ag:RSH. Nielson and Winge²¹ showed from metal reconstitution studies of the α and β domains of metallothionein that Ag(I) binds up to an initial stoichiometry of 6 Ag(I) in both α and β domains. Circular dichroism (CD) spectroscopy has proven to be very effective and precise in identifying structural changes in the metallothionein metal-binding sites as metals have been introduced.^{6,18,22-25} The metal:protein stoichiometry can be determined from the development of specific CD spectral signals. Silver(I) binding to apo-MT²² and to Zn₇-MT²⁵ has been investigated with CD spectroscopy by Zelazowski *et al.* Two species, Ag₁₂-MT 2 and Ag₁₈-MT 2, were characterized when up to 20 Ag(I) were added to the solution of apo-MT 2 at neutral pH and 55 °C. The only reported EXAFS result for silver(I)-containing metallothionein has been reported by Hasnain's group:²⁶ the Ag K-edge EXAFS result for Cd₂Ag₁₇-MT showed an average Ag-S bond length of 2.40 Å, with a coordination number of essentially 2 for the Ag(I).

As far as we know, no systematic studies of sulfur K-edge X-ray absorption spectroscopy on mammalian metallothioneins have been reported to date, although George and Winge have reported sulfur K-edge EXAFS data for yeast metallothionein.²⁷ In this paper, a comprehensive study on sulfur K-edge EXAFS spectra of Zn₇-MT, Cd₇-MT, Cu₁₂-MT, Ag₁₂-MT, and Ag₁₇-MT is presented. Two well-known metal-thiolate inorganic complexes, Cd₄(SPh)₁₀²⁻ and Zn₄(SPh)₁₀²⁻, are used to test the reliability of this technique. As the metal-containing metallothioneins are a complicated system, we use a circular dichroism technique to identify the well-defined structural species of Ag₁₂-MT 1 and Ag₁₇-MT 1. Then, the structural parameters are obtained from sulfur K-edge EXAFS data for

Ag₁₂-MT 1 and Ag₁₇-MT 1 related to the nature of the binding sites of silver-thiolate clusters in silver-containing metallothioneins. The unique advantage of this method is that the sulfur coordination environment can be directly obtained in the metal-binding sites in addition to the M-S bond lengths.

Materials and Methods

Zn₇-MT was isolated from the livers of rabbits following a series of 14 injections of a sterilized aqueous solution of ZnSO₄ (20 mg of Zn/kg of body weight) spread over a 2-week period and purified as described previously.^{6,21,28,29} Isoforms of Zn₇-MT 1 and Zn₇-MT 2 were separated by polyacrylamide gel electrophoresis as described previously.²⁸ Cd₇-MT and Cu₁₂-MT were prepared by replacement of Zn(II) in Zn₇-MT with Cd(II) and Cu(I), respectively. The process of replacement was monitored by CD spectroscopy for Cd₇-MT⁶ and emission spectroscopy for Cu₁₂-MT.³⁰ The free Zn(II) ions from Zn₇-MT were removed by Chelex-100.³¹ Apo-MT 1 was prepared from Zn₇-MT 1 by passing the protein down a Sephadex G-25 gel column, which had previously been equilibrated with a pH 2 acetic acid solution. Preparation of Ag₁₂-MT 1 and Ag₁₇-MT 1 was carried out by addition of Ag(I) as a form of AgNO₃ to apo-MT 1 at pH 3 and 50 °C; metal binding was monitored by the appearance of characteristic bands in the circular dichroism spectrum. The final metallothionein samples were concentrated by lyophilization. All preparations were carried out at room temperature and at neutral pH unless otherwise noted.

Protein concentrations were determined from measurements of SH groups using 5,5'-dithiobis(nitrobenzoic acid) in 6 M guanidine hydrochloride.³² Calculations were based on the assumption that 20 SH groups exist in the rabbit liver protein.²⁹ Metal concentrations were measured with a Varian 875 atomic absorption spectrometer.

Circular dichroism spectra were recorded on a Jasco J-500 spectrometer, controlled by an IBM 9001 computer using the program CDSCAN5.³³ The spectral data were organized and plotted on an HP 7550A plotter with the spectral data base program Spectra Manager³⁴ for the two-dimensional plots and with program PLOT3D³⁵ for the three-dimensional plots. The contour diagrams provide accurate values for peak maxima as a function of Ag:MT molar ratios.

X-ray absorption measurements were carried out on the Aladdin I GeV storage ring at the Canadian Synchrotron Radiation Facility (CSR), University of Wisconsin at Madison. Lyophilized solid samples were pressed lightly on a conducting tape for the X-ray absorption analysis. Sulfur K-edge EXAFS spectra were recorded from 30 eV below to 600 eV above the sulfur K-edge threshold energy (~2472 eV) on a double-crystal monochromator (DCM) in vacuum.³⁶ The beam was monochromatized using InSb crystals with a photon resolution of ~0.9 eV. The total electron yield (TEY) detection mode was used by directly monitoring the current from the sample. This mode of detection does not suffer from self-absorption. A careful study recently showed that the sampling depth of the TEY method is on the order of 70 nm at the Si K-edge.³⁷ This value is expected to be higher at the S K-edge. All spectra were normalized for I_0 , using an ionization chamber. The energy scale at the S K-edge was calibrated with reference to the strong absorption peak of elemental sulfur at 2472.0 eV. It was found that the relative energy scale was reproduced within 0.1 eV. The reported spectra are the average of five to nine scans. All data were collected at room temperature; the vacuum chamber was not equipped with a cryostat for low-temperature measurements.

The procedure of the data analysis was as follows. The EXAFS function is defined as $\chi(k) = [\mu(E) - \mu_0(E)]/\mu_0(E)$ where E and k are

- (17) Hasnain, S. S. *Top. Curr. Chem.* **1988**, *147*, 73-93.
 (18) Lu, W.; Zelazowski, A. J.; Stillman, M. J. *Inorg. Chem.* **1993**, *32*, 919-926.
 (19) Piotrowski, J. K.; Szymanska, J. A.; Mogilnicka, E. M.; Zelazowski, A. J. *Experientia, Suppl.* **1979**, *34*, 363-371.
 (20) Scheuhammer, A. M.; Cherian, M. G. *Toxicol. Appl. Pharm.* **1980**, *82*, 417-425.
 (21) (a) Winge, D. R.; Miklossy, K. A. *J. Biol. Chem.* **1982**, *257*, 3471-3476. (b) Nielson, K. B.; Winge, D. R. *J. Biol. Chem.* **1985**, *260*, 8698-8701.
 (22) Zelazowski, A. J.; Gasyna, Z.; Stillman, M. J. *J. Biol. Chem.* **1989**, *264*, 17091-17099.
 (23) Zelazowski, A. J.; Szymanska, J. A.; Law, A. Y. C.; Stillman, M. J. *J. Biol. Chem.* **1984**, *259*, 12960-12963.
 (24) Lu, W.; Stillman, M. J. *J. Am. Chem. Soc.* **1993**, *115*, 3291-3299.
 (25) Zelazowski, A. J.; Stillman, M. J. *Inorg. Chem.* **1992**, *31*, 3363-3370.
 (26) Hasnain, S. S.; Diakun, G. P.; Abrahams, I.; Ross, I.; Garner, C. D.; Bremner, I.; Vasak, M. *Experientia, Suppl.* **1987**, *52*, 227-236.
 (27) George, G. N.; Byrd, J.; Winge, D. R. *J. Biol. Chem.* **1988**, *263*, 8199-8203.

- (28) Zelazowski, A. J.; Szymanska, J. A.; Witas, H. *Prep. Biochem.* **1980**, *10*, 495-505.
 (29) Nielson, K. B.; Winge, D. R. *J. Biol. Chem.* **1984**, *259*, 4941-4946.
 (30) Green, A. R.; Presta, P. A.; Gasyna, Z.; Stillman, M. J. *Inorg. Chem.* **1994**, *33*, 4159-4168.
 (31) Cai, W.; Stillman, M. J. *Inorg. Chim. Acta* **1988**, *152*, 111-115.
 (32) Birchmeier, W.; Christen, P. *FEBS Lett.* **1971**, *18*, 208-213.
 (33) Gasyna, Z.; Browett, W. R.; Nyokong, T.; Kitchenham, B.; Stillman, M. J. *Chemom. Intell. Lab. Syst.* **1989**, *5*, 233-246.
 (34) Browett, W. R.; Stillman, M. J. *Comput. Chem.* **1987**, *11*, 73-80.
 (35) Gasyna, Z.; Stillman, M. J. Unpublished program.
 (36) Yang, B. X.; Middleton, F. H.; Olsson, B. G.; Bancroft, G. M.; Chen, J. M.; Sham, T. K.; Tan, K. H.; Wallace, D. *Nucl. Instrum. Methods* **1992**, *316*, 422-436.
 (37) Kasrai, M.; et al. Submitted to *Surf. Sci.*

the X-ray photon energy and the wavenumber of the photoelectron excited by the X-ray photon, respectively. $\mu_0(E)$ is the atomic absorption coefficient. The experimental energy origin is determined by the inflection point of the absorption threshold, $E_{\text{inflection}}$. The EXAFS spectra were extracted from the raw data using the standard procedure.³⁸ The pre-edge background was removed by the Victoreen function and the post-edge background was removed by a three-section cubic spline fit, and then the data were normalized by the edge jump with extrapolation of a straight-line fit above the edge. The contribution of resolved shell by Fourier transform in R -space corresponding to an absorber–scatterer interaction was back-transformed with a Fourier filter.

The data analysis was carried out using the nonlinear least-squares curve-fitting program EXAFIT.³⁹ The following expression was used to fit the data:

$$\chi(k) = \sum_j \frac{N_j}{k_j R_j^2} S_0^2 S(k_j) f_j(k_j) e^{-2k_j^2 \sigma_j^2} e^{-2R_j/\lambda} \sin[2k_j R_j + \Phi_j(k_j)]$$

where the sum is over all the neighboring atomic shells. R_j and N_j are respectively the mean internuclear distance between the central atom and atoms of the j th neighbor shell and the coordination number of the j th shell; $S_0^2 S(k)$ is a dimensionless function of k assigned to the reduction of the EXAFS signal due to multiple excitation effects; σ_j^2 (Debye–Waller factor) is the mean-squared relative displacement in R_j ; λ is the mean free path of the photoelectron due to the finite core hole lifetime and interactions with the valence electrons; $|f_j(k_j)|$ is the magnitude of the back-scattering amplitude of an atom in the j th shell; $\phi_j(k_j)$ is the scattering phase shift due to both the central and backscattering atoms; k_j is related to the experimental wavenumber of the photoelectron on the basis of the equation $k = [2m(E - E_{\text{inflection}})]^{1/2}/\hbar$ through the parameter ΔE_j defined as follows:

$$k_j = (k^2 - 0.2625\Delta E_j)^{1/2}$$

The effective backscattering amplitude $S_0^2 S(k_j) |f_j(k_j)| e^{-2k_j^2 \sigma_j^2} e^{-2R_j/\lambda}$ and phase shift $\phi_j(k_j)$ used for curve-fitting were calculated from an *ab initio* XAFS theory (FEFF)⁴⁰ in a single-scattering mode. S_0^2 has been shown to be insensitive to the chemical environment; therefore, it can be approximated by the corresponding atomic value.⁴¹ Throughout the analysis, $S_0^2 = 0.75$ was used. The curve-fitting was performed in both k -space on Fourier-filtered $k\chi(k)$ and in R -space on both the real and imaginary parts of the Fourier transform, and the results are quite consistent with each other. The average values obtained from both k - and R -space fitting were used as final results. In the curve-fitting for a single shell, four parameters, ΔE , R , $\Delta\sigma^2$, and N , were varied simultaneously, where $\Delta\sigma^2$ is the difference between the resulting σ^2 value and the constant input in the FEFF calculation. The residual sum of squares used in this work is defined as

$$\chi^2 = \frac{N_{\text{pts}}}{N_{\text{pts}} - n} \frac{1}{N} \sum_{j=1}^N (\text{data}_j - \text{model}_j)^2$$

where $N_{\text{pts}} = 1 + 2(\Delta k)\Delta R/\pi$ is the number of independent data points, n is the number of fitting parameters used, and N is the total number of data points. This is the quantity minimized in the nonlinear least-squares curve-fitting. The uncertainties of the results were estimated from the deviation of each parameter with its best-fit value (fixing this parameter and allowing all others to vary) which doubles the residual sum of squares between the fit and data.

Results

The unfiltered data in k - and R -space for $\text{Cd}_4(\text{SPh})_{10}^{2-}$, $\text{Cd}_7\text{-MT}$, $\text{Zn}_4(\text{SPh})_{10}^{2-}$, $\text{Zn}_7\text{-MT}$, $\text{Cu}_{12}\text{-MT}$, $\text{Ag}_{12}\text{-MT}$, and $\text{Ag}_{17}\text{-MT}$

(38) Sayer, D. E.; Bunker, B. A. In *X-ray Absorption: Principles, Application, Techniques of EXAFS, SEXAFS and XANES*; Koningsberger, D. C., Prins, R., Eds.; Wiley: New York, 1988; Chapter 6.

(39) Bauchspies, K. R. *Jpn. J. Appl. Phys., Suppl.* **1993**, *32*, 131–133.

(40) (a) Rehr, J. J.; Mustre de Leon, J.; Zabinsky, S. I.; Albers, R. C. *J. Am. Chem. Soc.* **1991**, *113*, 5135–5140. (b) Mustre de Leon, J.; Rehr, J. J.; Zabinsky, S. I.; Albers, R. C. *Phys. Rev. B* **1991**, *44*, 4146–4156.

(41) Stern, E. A. In *X-ray Absorption: Principles, Application, Techniques of EXAFS, SEXAFS and XANES*; Koningsberger, D. C., Prins, R., Eds.; Wiley: New York, 1988; p 40.

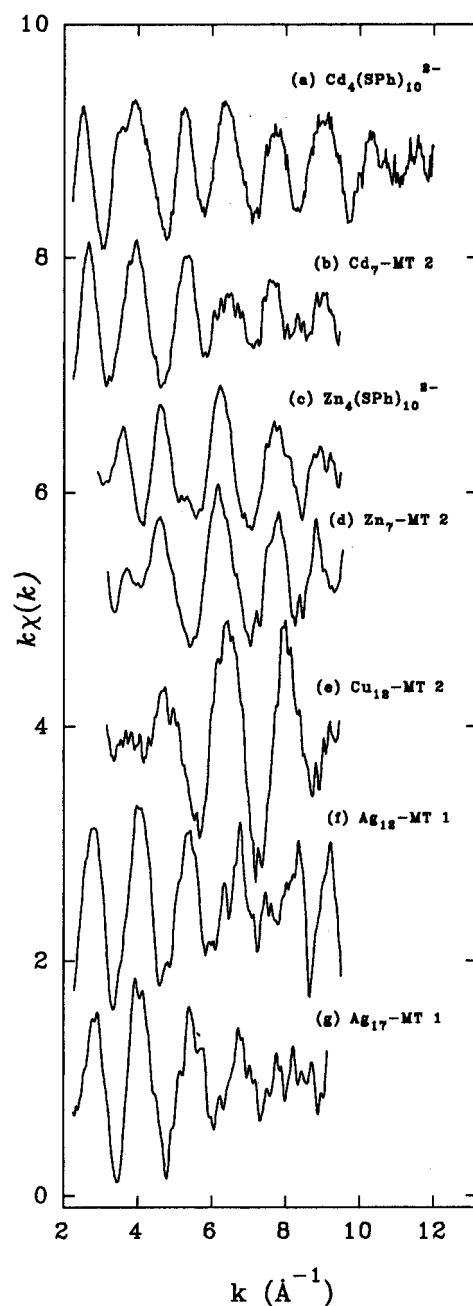


Figure 3. $k\chi(k)$ of model compounds and metallothioneins: (a) $\text{Cd}_4(\text{SPh})_{10}^{2-}$; (b) $\text{Cd}_7\text{-MT 2}$; (c) $\text{Zn}_4(\text{SPh})_{10}^{2-}$; (d) $\text{Zn}_7\text{-MT 2}$; (e) $\text{Cu}_{12}\text{-MT 2}$; (f) $\text{Ag}_{12}\text{-MT 1}$; (g) $\text{Ag}_{17}\text{-MT 1}$.

are shown in Figures 3 and 4, respectively. As all data were collected by sulfur K-edge EXAFS measurements, the overall spectra look quite complicated due to the fact that (i) two types of sulfurs (bridging and terminal) are bound to the metals and (ii) in addition to a dominant interaction between each sulfur and one or two metals, there are also S–C interactions. Because we are mainly interested in the local information about the sulfur–metal (S–M) shell, the data corresponding to the S–M shell in R -space were Fourier-filtered and analyzed by nonlinear least-squares curve-fitting. On the basis of the crystal structure of $\text{Cd}_4(\text{SPh})_{10}^{2-}$,⁴² the S–C bond length is about 1.8 Å, which is more than 0.4 Å away from that of the S–M shell (2.25–2.54 Å). Therefore, the two shells of S–C and S–M in R -space are practically distinguishable.⁴³ The EXAFS features of $\text{Zn}_4(\text{SPh})_{10}^{2-}$, $\text{Zn}_7\text{-MT}$, and $\text{Cu}_{12}\text{-MT}$, as shown in Figure 3,

(42) Hagen, K. S.; Holm, R. H. *Inorg. Chem.* **1983**, *22*, 3171–3174.

(43) Teo, B. K. In *EXAFS: Basic Principles and Data Analysis*; Jørgensen, C. K., et al., Eds.; Springer-Verlag: New York, 1986; p 127.

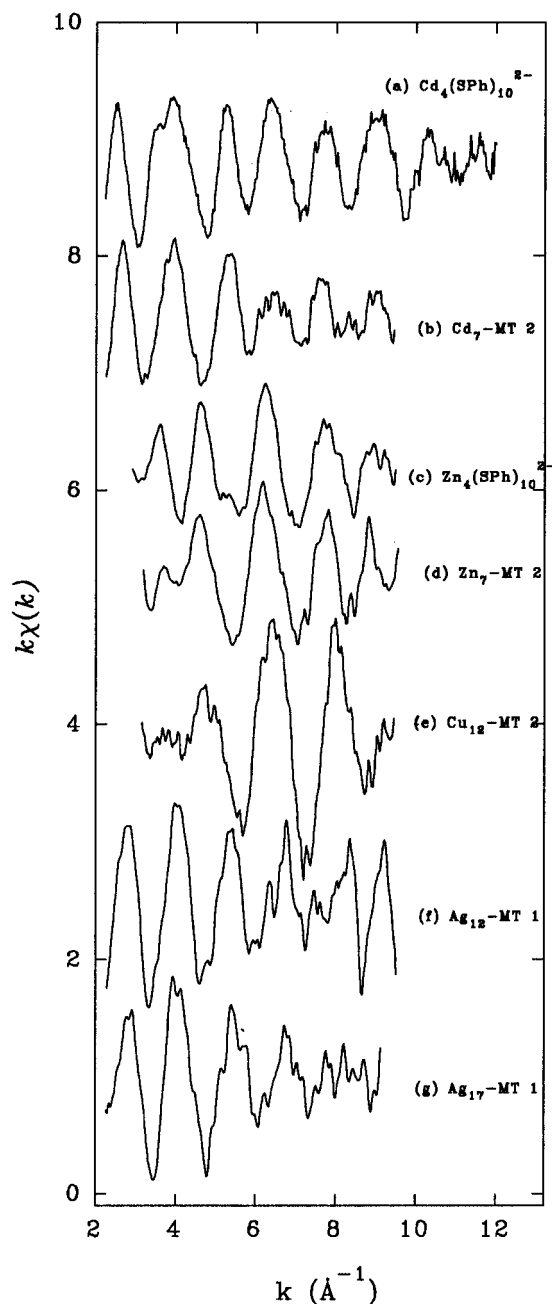


Figure 4. Magnitudes of the Fourier transforms of $k\chi(k)$. The positions of the peaks are shifted a few tenths of an angstrom from the actual interatomic distances because of the EXAFS phase shift. k -Space data ranges used in the transform: (a) $\text{Cd}_4(\text{SPh})_{10}^{2-}$, 2.22–12.05 \AA^{-1} ; (b) $\text{Cd}_7\text{-MT 2}$, 2.26–9.45 \AA^{-1} ; (c) $\text{Zn}_4(\text{SPh})_{10}^{2-}$, 2.92–9.50 \AA^{-1} ; (d) $\text{Zn}_7\text{-MT 2}$, 3.19–9.56 \AA^{-1} ; (e) $\text{Cu}_{12}\text{-MT 2}$, 3.15–9.45 \AA^{-1} ; (f) $\text{Ag}_{12}\text{-MT 1}$, 2.30–9.15 \AA^{-1} ; (g) $\text{Ag}_{17}\text{-MT 1}$, 2.27–9.13 \AA^{-1} .

are quite different from those of the heavy-metal-containing model complex and metallothioneins, $\text{Cd}_4(\text{SPh})_{10}^{2-}$, $\text{Cd}_7\text{-MT}$, $\text{Ag}_{12}\text{-MT}$, and $\text{Ag}_{17}\text{-MT}$. The magnitudes of all of the data in k -space, however, are more or less the same, implying that there is not much difference in sulfur coordination numbers in all compounds. As both terminal (coordination number is 1) and bridging (coordination number is 2) sulfurs are present in all compounds, the average coordination number of sulfur can be calculated on the basis of the expression

$$N(\text{S}) = x_t \times 1 + x_b \times 2$$

where x_t and x_b are the fractions of terminal and bridging sulfurs, respectively.

It is worth mentioning that the high end of the k value is limited to about 9.5 \AA^{-1} due to the presence of chloride in all

Table 1. Results of Nonlinear Least-Squares Curve-Fitting for All Complexes

complex	ΔE_0 (eV)	R (\AA)	$10^{-3}\sigma^2$ (\AA^2)	N	$10^{-5}G^a$
$\text{Cd}_4(\text{SPh})_{10}^{2-}$	0.5 ± 2.6	2.52 ± 0.02	4.7 ± 1.9	1.3 ± 0.4	0.754
$\text{Cd}_7\text{-MT 2}$	3.7 ± 1.4	2.54 ± 0.02	7.6 ± 3.3	1.2 ± 0.2	0.438
$\text{Zn}_4(\text{SPh})_{10}^{2-}$	8.1 ± 1.3	2.35 ± 0.03	7.1 ± 1.7	1.5 ± 0.3	0.341
$\text{Zn}_7\text{-MT 2}$	8.7 ± 1.2	2.34 ± 0.03	7.7 ± 1.4	1.4 ± 0.3	0.290
$\text{Cu}_{12}\text{-MT 2}$	3.0 ± 1.5	2.25 ± 0.01	4.8 ± 1.4	1.7 ± 0.2	0.875
$\text{Ag}_{12}\text{-MT 1}$	1.0 ± 1.7	2.45 ± 0.02	5.9 ± 3.4	1.4 ± 0.3	1.670
$\text{Ag}_{17}\text{-MT 1}$	2.5 ± 3.0	2.44 ± 0.03	9.8 ± 5.1	1.6 ± 0.5	1.290

^a For comparison, the goodness-of-fit is defined as χ_{min}^2 in R -space (see Materials and Methods).

samples, except $\text{Cd}_4(\text{SPh})_{10}^{2-}$, which was found to be chloride free. Chloride exhibits a strong K-edge absorption at about 2833 eV, which prevented us from analyzing the EXAFS data above 9.5 \AA^{-1} in k -space. Therefore, the error in the coordination number of sulfur calculated from these EXAFS data may be a little larger than usual. The S–M bond lengths, however, can be estimated quite precisely. Considering the limited k -space data range and the room temperature at which the samples were measured, it is very difficult to analyze the weak EXAFS features for higher shells in R -space; thus no attempt was made to quantitatively analyze the higher shell scatterers, such as S··S interactions. We also noticed that the EXAFS signal for S–C is not really shown in Figure 4 for all samples except for $\text{Cd}_4(\text{SPh})_{10}^{2-}$. This may be due partly to the fast decay in amplitude of the carbon atom.

The sulfur K-edge XANES spectra of all samples were also examined to find information regarding the bridging and terminal sulfurs in proteins. The formal chemical state of sulfur in all of the model and protein samples is S^{2-} . Since the line width at the K-edge is rather broad (~ 2 eV), small differences in the chemical shifts could not be observed. The sulfur K-edge spectra of several organic compounds have been reported before and indicated the limitation of the sulfur K-edge technique.⁴⁴

Sulfur K-Edge EXAFS Spectra of $\text{Cd}_4(\text{SPh})_{10}^{2-}$ and $\text{Cd}_7\text{-MT}$. The unfiltered sulfur K-edge spectra in k - and R -space for $\text{Cd}_4(\text{SPh})_{10}^{2-}$ and $\text{Cd}_7\text{-MT}$ are shown in Figure 3a,b and Figure 4a,b, respectively. They are very similar except that the data range for the protein is shorter. The filtered data responsible for the S–Cd interactions were analyzed by curve-fitting in both k - and R -space, and the fitting results are shown in Figure 5a,b (see Supporting Information) for $\text{Cd}_4(\text{SPh})_{10}^{2-}$ and in Figure 5c,d for $\text{Cd}_7\text{-MT}$, respectively. All fitted parameters are summarized in Table 1. There are two peaks, one dominant and the other minor, exhibited in R -space even when there is only a single shell (S–Cd), as revealed by Figure 5b,d. This phenomenon, as a result of the Ramsauer–Townsend effects, partly explains why the $k\chi(k)$ data in k -space in Figure 3 look so complicated. The Cd–S bond lengths were estimated from the nonlinear least-squares curve-fitting to be 2.52 ± 0.02 \AA for $\text{Cd}_4(\text{SPh})_{10}^{2-}$ and 2.54 ± 0.02 \AA for $\text{Cd}_7\text{-MT}$. The coordination numbers of sulfur in the Cd(II) model compound and the protein are 1.3 ± 0.4 and 1.2 ± 0.2 , respectively. Significantly, the results for $\text{Cd}_4(\text{SPh})_{10}^{2-}$ obtained by this method are in agreement with the average Cd–S bond distance (2.54 \AA), based on the individual Cd–S bond distances from the single-crystal X-ray diffraction,⁴² and also with the value of the Cd–S bond distance (2.54 \AA) derived from Cd K-edge EXAFS measurements.⁴⁵ Correspondingly, the Cd–S bond distance in $\text{Cd}_7\text{-MT}$ from our EXAFS data is also consistent with the reported values of 2.50–2.53 \AA from Cd K-edge EXAFS.^{9,10} The calculated average coordination numbers of

(44) Kasrai, M.; et al. *Geochim. Cosmochim. Acta* **1994**, *58*, 2865–2872.

(45) Stephan, D. W.; Hitchcock, A. P. *Inorg. Chim. Acta* **1987**, *136*, L1–L5.

Table 2. Summary of Structural Parameters from Previous Work and This Work

complex	$R(M-S)$ (Å)		$N(S)$		$N(M)^k$	geometry
	previous work	this work	calcd ^g	this work		
$Cd_4(SPh)_{10}^{2-}$	2.54 ^a	2.52 ± 0.02	1.6	1.3 ± 0.4	4	tetrahedral
Cd_7-MT	2.50–2.53 ^b	2.54 ± 0.02	1.4	1.2 ± 0.2	4	tetrahedral
$Zn_4(SPh)_{10}^{2-}$	2.35 ^c	2.35 ± 0.03	1.6	1.5 ± 0.3	4	tetrahedral
Zn_7-MT	2.33–2.35 ^d	2.34 ± 0.03	1.4	1.4 ± 0.3	4	tetrahedral
$Cu_{12}-MT$	2.24–2.25 ^e	2.25 ± 0.01	1.8 ^h	1.7 ± 0.2	3	trigonal
$Ag_{12}-MT$	N/A	2.45 ± 0.02	1.2 ⁱ	1.4 ± 0.3	2	digonal
$Ag_{17}-MT$	2.40 ^f	2.44 ± 0.03	1.7 ^f	1.6 ± 0.5	2	digonal

^a From refs 42 and 45. ^b From refs 9 and 10. ^c From ref 46. ^d From refs 47 and 9. ^e From refs 48 and 13. ^f From ref 26. ^g The average coordination number of sulfur for each compound is calculated on the basis of the equation $N(av) = x_t \times 1 + x_b \times 2$, where x_t is the fraction of the terminal sulfurs and x_b is the fraction of the bridging sulfurs. ^h This number is derived on the basis of the proposed model in our group (see ref 48). ⁱ This number is calculated on the basis of the model where 4 bridging and 16 terminal sulfurs are present in $Ag_{12}-MT$. ^j This number is calculated on the basis of the model where 14 bridging and 6 terminal sulfurs are present in $Ag_{17}-MT$. ^k The coordination number of the metal for each compound is obtained either from the well-characterized structure ($Cd(II)$ and $Zn(II)$ compounds) or on the basis of the $M-S$ bond distances from sulfur K-edge EXAFS measurements ($Cu(I)$, $Ag(I)$ proteins).

sulfurs for these two compounds are given in Table 2. The coordination numbers of sulfur obtained from this work for both samples are also quite reasonable, measured as 1.3 compared with the calculated values of 1.6 for $Cd_4(SPh)_{10}^{2-}$ (x_t and x_b are 0.4 and 0.6, respectively) and measured as 1.2 compared with the calculated value of 1.4 for Cd_7-MT (x_t and x_b are 0.6 and 0.4, respectively).

Sulfur K-Edge EXAFS Spectra of $Zn_4(SPh)_{10}^{2-}$ and Zn_7-MT 2. Figure 3c,d shows the $k\chi(k)$ data for $Zn_4(SPh)_{10}^{2-}$ and Zn_7-MT , respectively. As in the case of $Cd_4(SPh)_{10}^{2-}$ and Cd_7-MT , these two spectra also look very similar. From these unfiltered data it is expected that a dominant single shell exists in both compounds. This is more clearly displayed in the Fourier transforms in Figure 4c,d. The filtered data and the curve-fitting in both k - and R -space are shown in Figure 6a,b (see Supporting Information) for $Zn_4(SPh)_{10}^{2-}$ and in Figure 6c,d for Zn_7-MT , respectively. The fitting results are given in Table 1. Unlike $Cd_4(SPh)_{10}^{2-}$ and Cd_7-MT , for which two peaks are observed in the R -space responsible for the $S-Cd$ shell, $Zn_4(SPh)_{10}^{2-}$ and Zn_7-MT yield only one peak in the specified R -space. The $Zn-S$ bond lengths from curve-fitting are calculated to be 2.35 ± 0.03 and 2.34 ± 0.03 Å for $Zn_4(SPh)_{10}^{2-}$ and Zn_7-MT , respectively. Again, these results agree well with the values from the X-ray diffraction⁴⁶ of $Zn_4(SPh)_{10}^{2-}$ (2.35 Å) and previous Zn K-edge EXAFS spectra of Zn_7-MT (2.34–2.35 Å).^{9,47} The coordination numbers of sulfur calculated from the EXAFS data are 1.5 ± 0.3 for $Zn_4(SPh)_{10}^{2-}$ and 1.4 ± 0.3 for Zn_7-MT . These numbers are also close to the theoretical values, shown in Table 2, of 1.6 for $Zn_4(SPh)_{10}^{2-}$ and 1.4 for Zn_7-MT , based on the well-characterized structures of these two compounds.

Sulfur K-Edge EXAFS Spectrum of $Cu_{12}-MT$ 2. Both CD and emission spectroscopies display a steady development of a signal that exhibits a maximum intensity at a $Cu:MT$ stoichiometric ratio of 12, when $Cu(I)$ is gradually added to Zn_7-MT 2 in aqueous solutions.^{30,48} Sulfur K-edge EXAFS measurements were carried out in order to further probe the local structure of the Cu -thiolate clusters in copper metallothionein based on a correlation of the bond distance with the coordination geometry. The $k\chi(k)$ of $Cu_{12}-MT$ is shown in Figure 3e, and the unfiltered data in R -space are shown in Figure 4e. The single-shell curve-fittings of the main peak in the Fourier transform are shown in Figure 7a,b in k - and R -space, respectively, and the values obtained are summarized in Table 1. The $Cu-S$ bond length in $Cu_{12}-MT$ obtained from analysis of the EXAFS data is 2.25

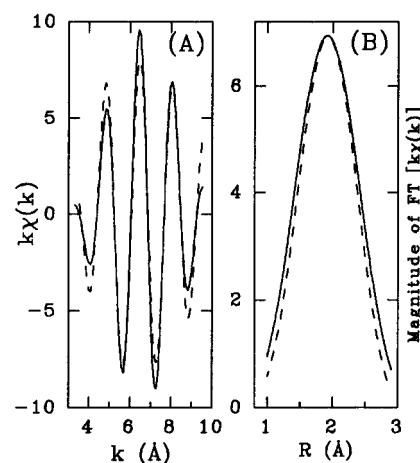


Figure 7. (A) $k\chi(k)$ of Fourier-filtered (solid) and the fit (dotted) data. (B) Magnitudes of the Fourier transform (solid) and the fit (dotted) in R -space. Both (A) and (B) are for $Cu_{12}-MT$ 2, where the filtering window range is 1.05–2.75 Å.

± 0.01 Å, which is consistent with the results from the Cu K-edge absorption measurements.^{13,14} The relatively high coordination number of sulfur (1.7 ± 0.2) means that a high fraction of bridging sulfurs is present in the copper-thiolate cluster, which is in good agreement with the average coordination number of sulfur (given in Table 2) of 1.8 based on the recently proposed model for $Cu_{12}-MT$ 2 from our group (x_t and x_b are 0.2 and 0.8, respectively).⁴⁸

Circular Dichroism Spectrum of Silver(I) Metallothionein.

CD spectra recorded during titration of metallothioneins with metals have previously been used to provide essential information on the metal to protein stoichiometric ratio for species not readily identified by other techniques.^{6,18,22–25} Analysis of the CD spectra obtained during a titration of Zn_7-MT 2 with $Ag(I)$ ²⁵ showed that the presence of $Zn(II)$ in Zn_7-MT 2 inhibited formation of $Ag_{12}-MT$ 2. In the present work, CD spectra were measured as up to 19 $Ag(I)$ were gradually added to apo-MT 1. Apo-MT 1 was prepared by passing Zn_7-MT 1 down a Sephadex G-25 gel column equilibrated with a pH 2 acetic acid solution to remove $Zn(II)$. Acetic acid was used instead of hydrochloric acid to avoid the possible interaction between Cl^- and the incoming $Ag(I)$. We found that the CD spectral intensity for the range of Ag_n-MT species ($n = 1-19$) is strong even at a pH as low as 3. This is in direct contrast to metal-containing metallothioneins such as $Zn-MT$ and $Cd-MT$. The intensities of many of the characteristic bands in the CD spectrum of Ag_n-MT 1 are dependent on both the pH and the temperature. Particularly, the CD spectral profile of $Ag_{12}-MT$ is much better resolved when the CD spectra were recorded at 50 °C rather than room temperature. $Ag(I)$ was added to a single portion of

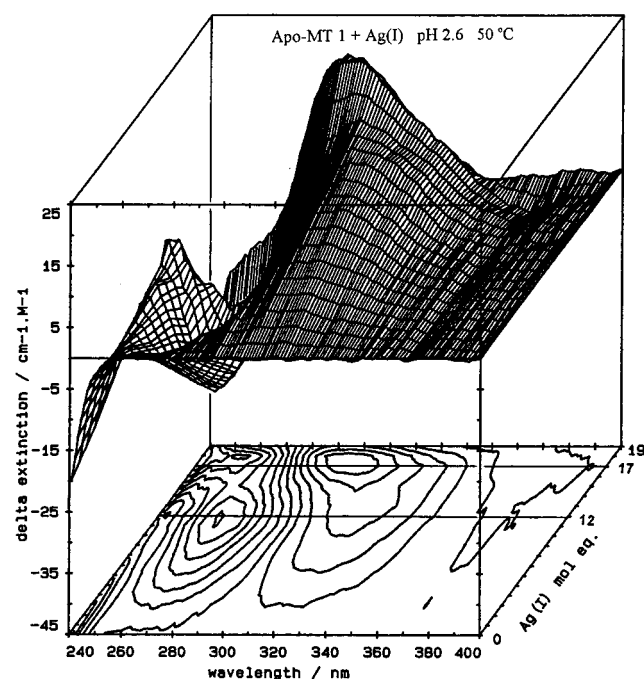
(46) Hancher, J. L.; Khan, M.; Said, F. F.; Tuck, D. G. *Polyhedron* **1985**, *4*, 1263–1267.

(47) Garner, C. D. *Adv. Inorg. Chem.* **1991**, *36*, 319–320.

(48) Presta, P. A.; Green, A. R.; Zelazowski, A. J.; Stillman, M. J. *Eur. J. Biochem.* **1995**, *227*, 226–240.

Table 3. CD Spectral Features of Ag-MT 1 Species Formed from apo-MT 1 at pH 2.7 and 50 °C

protein used	metal added	species formed	CD spectral features
apo-MT 1	Ag(I)	Ag ₁₂ -MT 1	263 nm (−, very strong), 314 nm (+, strong); after 12 Ag(I), the band at 263 nm disappears and the band at 314 nm is gradually shifted to higher energy
apo-MT 1	Ag(I)	Ag ₁₇ -MT 1	302 nm (+, very strong), 370 nm (−, weak); after 17 Ag(I), the band at 302 nm collapses and the intensity of the band at 370 nm decreases

**Figure 9.** Three-dimensional CD spectra for a solution of apo-MT 1 with Ag(I):MT from 0 to 19 recorded at pH 2.7 and 50 °C. The grid lines added to the contour diagram are drawn for Ag(I) molar ratios of 12 and 17, respectively.

apo-MT 1 at pH 3, rather than to the different solutions with each containing an increasing equivalent number of Ag(I) in order to keep the CD spectrum as consistent as possible. Figure 8 (see Supporting Information) shows the two-dimensional CD spectra recorded for a single solution of apo-MT 1 with an increasing molar ratio of Ag(I):MT 1, from 0 to 12 (a) and from 12 to 19 (b). As shown in Figure 8a, the CD bands at 263 nm (−, very strong) and 314 nm (+, strong) intensified continuously as up to 12 Ag(I) were added to the solution of apo-MT 1. When from 12 to 17 Ag(I) were further added to the solution of apo-MT 1 as seen in Figure 8b, the negative CD band at 263 nm disappeared, and a new CD feature appeared, which is characterized by bands at 302 nm (+, very strong) and 370 nm (−, weak) at the 17 Ag(I) point. In addition, a blue shift of the CD maximum, which was located at 314 nm (+) with 12 Ag(I) and at 302 nm (+) with 17 Ag(I), takes place. These significant changes, namely, the disappearance of the band at 263 nm (−), the blue shift of the band from 314 to 302 nm, and the new weak band near 370 nm (−), clearly indicate that three-dimensional structural changes take place between the 12 Ag(I) and the 17 Ag(I) points. When more than 17 Ag(I) are added, the CD signal simply collapses, indicating that the chirality of the Ag(I)–thiolate cluster structure in Ag-MT 1 decreases. The CD features observed when Ag(I) is added to apo-MT 1 at low pH and 50 °C are summarized in Table 3. Figure 9 shows a three-dimensional view of the CD spectra with the *z* axis representing the molar ratio of Ag(I):MT 1. Using the three-dimensional surfaces and contour plot, the speciation which develops in the course of the titration with Ag(I) can be easily identified. The CD analysis unambiguously indicates that both Ag₁₂-MT 1 and Ag₁₇-MT 1 are formed in the course of the titration but that only minor coordination changes take place

around the metal between the *n* = 12 and *n* = 17 points, unlike the case with Cu(I).⁴⁸

Sulfur K-Edge EXAFS Spectra of Ag₁₂-MT 1 and Ag₁₇-MT 1. As indicated by the CD spectra, two species, Ag₁₂-MT 1 and Ag₁₇-MT 1, are formed during addition of Ag(I) to apo-MT 1 at about pH 3 and 50 °C. Solid samples of Ag₁₂-MT 1 and Ag₁₇-MT 1 were prepared under these conditions. During the preparation, Ag(I) binding was monitored by ensuring that the CD spectra recorded were the same as those shown in Figure 8. Great care was taken to ensure that the number of silver(I) ions added did not pass 12 or 17, respectively, during the preparation.

The $k\chi(k)$ of Ag₁₂-MT 1 and Ag₁₇-MT 1 in *k*-space are shown in Figure 3f,g, and the unfiltered data in *R*-space are shown in Figure 4f,g, respectively. By looking at these data, one can see that (i) the frequencies of the oscillations are almost the same, meaning that the Ag–S bond lengths in these two protein complexes are more or less the same, and (ii) as with the Cd(II) compounds, the complexity of the EXAFS oscillation features in *k*-space implies that more than one peak corresponding to the Ag–S shell is expected in *R*-space. This is due to the scattering of the heavy scatterer such as silver. The filtered data and curve-fitting results in both *k*- and *R*-space are shown in Figure 10a,b for Ag₁₂-MT 1 and in Figure 10c,d for Ag₁₇-MT 1, respectively. The fitted results are also given in Table 1. As expected from the *k*-space data, the Ag–S bond lengths are almost the same, 2.45 ± 0.02 Å for Ag₁₂-MT 1 and 2.44 ± 0.03 Å for Ag₁₇-MT 1. *On the basis of the correlation between Ag–S bond lengths and the adopted Ag(I) geometry from the Ag–thiolate model compounds,⁴⁹ the bond lengths for the proteins suggest that the Ag(I) adopts a digonal geometry in both proteins.* The average coordination numbers of sulfur are estimated to be 1.4 ± 0.3 for Ag₁₂-MT 1 and 1.6 ± 0.5 for Ag₁₇-MT 1. These results clearly indicate that the local structures of the Ag(I)–thiolate clusters are very similar in these two silver-containing metallothioneins. The lack of change in the S–Ag distance with the digonal coordination in both Ag₁₂-MT 1 and Ag₁₇-MT 1 implies that the fraction of bridging sulfur in Ag₁₇-MT 1 is higher than that in Ag₁₂-MT 1.

Discussion

The structure of the M₇-MT species, M = Cd(II) and Zn(II), is well established,^{3–6} with each metal tetrahedrally coordinated to four cysteinyl sulfurs, either terminal or bridging, in two binding domains based on M₄S₁₁ (α) and M₃S₉ (β) stoichiometries. Chemical analysis²¹ and spectroscopic titrations^{1c,6,22} have determined a metal to MT 2 stoichiometric ratio between Cu(I) and mammalian apometallothionein of 12:1. Spectroscopic titrations have also indicated a complex with a Cu(I):MT 2 ratio of 15.⁴⁸ Similar titrations for Ag(I) (see Figure 9) suggest stoichiometric Ag(I):MT 1 ratios of 12 and 17. The details of the structure of the M_{12–17}S₂₀ cluster species (M = Cu(I), Ag(I)) are not well-known. Generally, when the metal is bound to the metallothionein, there exists a corresponding three-dimensional structure, for example, involving trigonal or digonal coordination of the metal by the cysteinyl sulfurs. The

(49) Tang, K.; Aslam, M.; Block, E.; Nicholson, T.; Zubieta, J. *Inorg. Chem.* **1987**, *26*, 1488–1497.

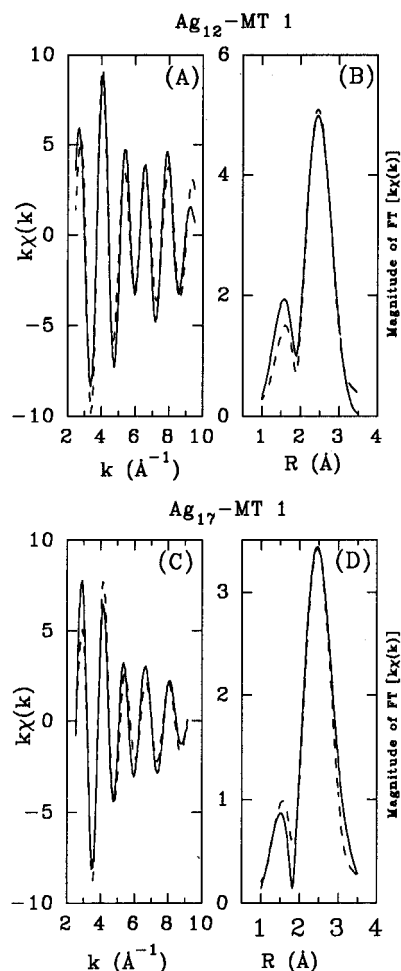


Figure 10. Left: $k\chi(k)$ of Fourier-filtered (solid) and the fit (dotted) data. Right: Magnitudes of the Fourier transform (solid) and the fit (dotted) in R -space. (A) and (B) are for Ag_{12} -MT 1, where the filtering window range is 1.30–2.95 Å; (C) and (D) are for Ag_{17} -MT 1, where the filtering window range is 1.35–3.03 Å.

EXAFS data in this study were recorded from proteins with precise bound–metal:MT stoichiometric ratios established by either CD or emission spectral data.

In general, EXAFS spectroscopy can provide accurate measurements of distances between the absorber and surrounding scatterers, which can be used to determine the local structure of the system of interest. It is especially advantageous to apply this technique to biological compounds for which no X-ray crystallographic data are available or for which they are only available at low resolution. A major advantage of measuring sulfur K-edge absorption spectra in this study is that the metal-binding sites for a number of different metals can be compared directly from the sulfur environment. Conditions for the measurements remain the same, so that observed changes can be interpreted specifically in terms of changes in metal–sulfur bond lengths and coordination geometries. The unique feature of the sulfur K-edge data is that they provide information about the coordination of the sulfur bound to metals, which is unavailable by other techniques. Moreover, when chloride is not present, such as in the case of model compounds, a long range of K -space can be recorded, which can provide S–S distances. This may become useful in model compound characterization.

The fact that the metal–sulfur bond lengths in Cd(II) and Zn(II) model compounds are in good agreement with the values reported by both X-ray diffraction data^{42,46} and metal K-edge EXAFS measurements^{8,45} means that the sulfur K-edge absorption method is reliable. The results for Zn₇- and Cd₇-MT from

Table 4. Summary of the Range of M–S (M = Cu, Ag) Bond Lengths (Å) in Metal–Thiolate Compounds

	digonal	trigonal	tetrahedral
copper(I)–thiolate compounds ^a	2.15–2.17	2.24–2.27	2.30–2.42
silver(I)–thiolate compounds ^b	2.38–2.44	2.50–2.58	2.55–2.65

^a Data taken from refs 54–57. ^b Data taken from refs 49, 60, and 63.

sulfur K-edge EXAFS measurements in this work are also consistent with the previously reported findings.^{9,10,47}

Copper binds to metallothionein exclusively in the form of Cu(I), with the d^{10} configuration. Direct evidence for this comes from EPR,⁵⁰ XPS,⁵¹ luminescence,^{30,52} and the lack of a d–d transition optical spectroscopy.⁵³ Although it is generally believed that copper in metallothionein adopts low coordination numbers (2 or 3), rather than 4 as in the case of Cd(II) and Zn(II), a complete description of the cluster structure is not yet available, as no X-ray structural analysis has been described. The Cu_{12} -MT species can be characterized by a maximum at 600 nm in the optical emission spectrum³⁰ and a distinctive derivative feature in the CD spectrum.⁴⁸ Sulfur K-edge EXAFS measurements provide the necessary information on the local structure for the copper–thiolate clusters in Cu_{12} -MT. It has been previously reported that the Cu–S bond lengths for Cu(SR)₂ (CN = 2), Cu(SR)₃ (CN = 3), and Cu(SR)₄ (CN = 4) centers for inorganic model compounds are approximately 2.15–2.17, 2.24–2.27, and 2.30–2.42 Å, respectively,^{54–57} as shown in Table 4. The Cu–S bond length of 2.25 Å in Cu_{12} -MT 2 reported here indicates that the Cu(I) in Cu_{12} -MT from rabbit liver metallothionein is coordinated to three sulfurs with a trigonal geometry. Pickering and co-workers¹⁴ proposed that there exists 30% digonal copper(I) in rat liver Cu- β MT on the basis of a correlation between the average Cu–S bond length obtained from an EXAFS curve-fitting analysis and the data from a number of synthetic copper(I)–thiolate cluster crystal structures. Although we cannot rule out this possibility at this stage, there are several points that can be noted. (i) The assumption that silver-containing metallothionein is analogous to the copper protein is clearly not strictly true in terms of the local structure of these two metal–thiolate clusters. While in some inorganic compounds Cu(I) and Ag(I) adopt similar environments, silver(I)–thiolate clusters with digonal geometry are more common than those with trigonal coordination whereas copper prefers trigonal coordination in copper(I)–thiolate compounds. Significantly, Cu(I) and Ag(I) binding to MT are not the same. Cu(I) forms the very well-defined Cu_{12} -MT species in which a three-dimensional structure based on copper–thiolate clusters forms. With Cu(I):MT > 15, the optical data^{30,48} show that the protein unwinds. On the other hand with Ag(I), both Ag_{12} -MT and Ag_{17} -MT form as shown in Figure 9 with CD spectral profiles different from that of Cu-MT.⁴⁸ (ii) According to the proposed correlation, it can be seen that the choice of R_f (the distance for trigonal Cu–S) and R_d (the distance for digonal Cu–S) is very critical. As the Cu–S bond lengths in different synthetic copper(I)–thiolate compounds with

(50) Geller, B. L.; Winge, D. R. *Arch. Biochem. Biophys.* **1982**, *213*, 109–117.

(51) Weser, U.; Hartmann, H. J.; Fretzdorff, A.; Strobel, G. J. *Biochim. Biophys. Acta* **1977**, *493*, 465–477.

(52) Byrd, J.; Berger, R. M.; McMillan, D. R.; Wright, C.; Hamer, D.; Winge, D. R. *J. Biol. Chem.* **1988**, *263*, 6688–6694.

(53) Lerch, K.; Beltrami, M. *Chem. Scr.* **1983**, *21*, 109–115.

(54) Dance, I. G. *Aust. J. Chem.* **1979**, *31*, 2195–2206.

(55) Griffith, E. H.; Hunt, G. W.; Amma, E. L. *J. Chem. Soc., Chem. Commun.* **1976**, 432–433.

(56) Birker, P. J. M. W. L.; Freeman, H. C. *J. Am. Chem. Soc.* **1977**, *99*, 6890–6899.

(57) Hollander, F. J.; Coucouvanis, D. *J. Am. Chem. Soc.* **1974**, *96*, 5646–5648.

the same geometry vary to some extent (see Table 4 and ref 58), the question may then become, Are the Cu–S bond lengths of 2.28 and 2.16 Å typical of trigonal and digonal coordinations, respectively? (iii) In spite of the fact the EXAFS spectroscopy can provide accurate bond lengths of the shell of interest, an error of 0.01–0.03 Å in the estimation of bond lengths is common, depending on the quality of data, the available k range. The difference in Cu–S bond lengths between R_{av} for rat liver Cu β -MT (2.255 Å) and R_l (2.28 Å) is only 0.025 Å. Hence, we must ask if this difference in bond lengths is entirely due to the digonal fraction of copper(I) in the protein.

NMR data for the Ag_7S_{10} cluster in Ag-MT from yeast (a single-domain structure compared with the two-domain structure in rabbit liver MT, that is the form of this present study) have been interpreted⁵⁹ in terms of a mixture of digonally and trigonally bound Ag(I). These results were transferred to the associated Cu-MT structure for which no NMR connectivity data could be obtained. However, for the mammalian two-domain protein, the CD titration data⁴⁸ clearly show that $Cu_{12}S_{20}$ clusters form as a distinct species, whereas the $Ag_{12}S_{20}$ cluster appears to be a part of a reaction that forms in sequence Ag_{17} -MT 1. The similarity in EXAFS parameters for Ag_{12} -MT 1 and Ag_{17} -MT 1 (Table 1) coincides with the interpretation that the CD spectrum for Ag_{12} -MT 1 supports a structure that involves digonal Ag(I), whereas in Cu-MT, the Cu(I) is mainly trigonal.

Recent studies in our group suggest that the presence of digonal Cu(I) in *Saccharomyces cerevisiae* Cu-MT may be confirmed by observation of the 340 nm band in the CD spectra of the purified yeast protein (unpublished results) and of rabbit liver Cu_{15} -MT.⁴⁸ This band, however, is not seen in the CD spectrum of rabbit liver Cu_{12} -MT, which we propose precludes the possibility of a significant fraction of digonal coordination in this protein. A model for Cu_{12} -MT has been proposed by our group.⁴⁸ The structure of Cu_6S_9 in the β domain is similar to that proposed by Winge's group¹³ with all 6 coppers binding to 9 bridging cysteinyl sulfurs trigonally. Replacement of two bridging cysteinyl thiolates in the M_7 -MT α domain with 4 terminal thiolate ligands gives rise to the structure for the α domain of Cu_6 -MT in which 6 coppers bind to 11 sulfurs through trigonal coordination in a bicyclo arrangement similar to the α domain in M_7 -MT except that two 8-membered rings are involved instead of two 6-membered rings in M_7 -MT. The calculation was carried out using the CAChe system, and the results show that each Cu(I) in Cu_{12} -MT is exclusively trigonally coordinated; the average Cu–S bond length is 2.24 Å, and an average coordination number for the sulfur is 1.8, which are in close agreement with the results obtained from our current sulfur K-edge EXAFS measurements.

The silver metallothionein species described in this paper are characterized by saturation in the chiral intensity as the Ag(I):S ratio increases. The CD method used for identification of metal-MT is essential in that the stoichiometric metal:S ratio completely controls the cluster structure of the protein. The sharp and specific CD spectrum indicates the formation of a well-defined metal–thiolate cluster. Because the apo-MT 1 adopts a random-coil structure,⁶ there is no contribution to the CD spectrum in the 230–400 nm range from the peptide itself. This implies that the intrinsic chirality of the amino acids does not contribute to the CD signals recorded between 230 and 400 nm. The CD spectrum arises exclusively from a chiral nature

of the protein adapted by the silver-binding site. We report that formation of Ag_{12} -MT 1 and Ag_{17} -MT 1 is more complete and the spectral signatures are better resolved in the CD spectrum when Ag(I) is added to apo-MT 1 at low pH values than when Ag(I) is added to Zn_7 -MT 1 at neutral pH.²⁵ This may be because the presence of Zn(II) in metallothionein precludes the formation of Ag_{12} -MT 1 through competition between the original tetrahedrally coordinated Zn(II) and the incoming Ag(I), which tends to change the previous geometry, as in the case in which the presence of Cd(II) in Cd_7 -MT inhibits formation of a three-dimensional structure for Hg_7 -MT.²⁴ It has been suggested²² that at higher temperatures the protein can exert domain specificity in such a way that completely filled domains are formed rather than mixture of complexes. This contrasts with the kinetic product formed at room temperature and below, in which metals are bound across the peptide chain and more likely to form random cross-linked regions in place of the well-defined clusters. Titration of apo-MT 1 with Ag(I) carried out at higher temperature (50 °C) indeed gave much better resolved CD spectra for Ag_{12} -MT 1 than that carried out at room temperature. As shown in Figure 8a and Figure 9, the flatness of the first spectrum recorded without any Ag(I) present between 240 and 400 nm confirms that the intrinsic chirality of the peptide chain in apo-MT 1 does not produce any CD signal in the recorded wavelength range. When up to 12 Ag(I) are added, a derivative band with a maximum at 314 nm and a minimum at 263 nm develops and intensifies continuously as shown in Figure 9, implying that a distinct silver metallothionein cluster with a specific three-dimensional structure as a whole forms. When the Ag(I):MT ratio reaches 17 in MT 1 as shown in Figure 8b, a new CD profile is seen: the negative peak at 263 nm vanishes, the 314 nm band blue-shifts to 302 nm, and a new weak negative band at 370 nm appears. These significant changes unambiguously indicate that considerable modification takes place as the Ag(I):MT 1 molar ratio increases from 12 to 17. These new characteristic CD features indicate that another Ag-MT species forms which is different from Ag_{12} -MT 1. The blue shift of the band implies an increase in the ligand to metal charge transfer (LMCT) transition energy, through either stabilization of ground state energy level or destabilization of the excited state energy. The peptide chain must rearrange in such a way to accommodate the increased Ag(I)–thiolate bonding with the 17 Ag(I). When more than 17 Ag(I) are introduced, the CD intensity simply collapses, indicating the loss of chirality from the Ag(I)–thiolate cluster due to the destruction of the tertiary structure.

The information provided by CD spectroscopy during the titration leads us to question what kinds of modifications give rise to these remarkable changes in the CD spectra between 12 Ag(I) and 17 Ag(I). One possibility, which has been proposed previously, is that the coordination geometry of Ag(I) and hence the corresponding tertiary structure are changed from trigonal in Ag_{12} -MT 1 to digonal in Ag_{17} -MT 1. The difference in CD spectra between Ag_{12} -MT 1 and Ag_{17} -MT 1 could also arise mainly from changes in the tertiary structure without change in the coordination geometry. However, the information provided by the CD spectra is not sensitive to the coordination around the metal, just the structure of the entire metal-binding site. Sulfur K-edge EXAFS spectroscopy is particularly useful in providing the required complementary information about the local structure in the silver(I)–thiolate clusters.

The EXAFS data features in both k - and R -space shown in Figures 3f,g and 4f,g, respectively, suggest that the local structures of the silver(I)–thiolate binding sites in Ag_{12} -MT 1 and Ag_{17} -MT 1 are in fact similar. The Ag–S bond lengths obtained from curve-fitting are 2.45 ± 0.03 Å for Ag_{12} -MT 1

(58) Stillman, M. J.; Presta, A.; Gui, Z.; Jiang, D. In *Metal-based Drugs*; Gielen, M., Ed.; Freund Publishing House Ltd.: London, 1994; Vol 1, pp 375–393.

(59) (a) Narula, S. S.; Winge, D. R.; Armitage, I. M. *Biochemistry* **1993**, *32*, 6773–6787. (b) Narula, S. S.; Mehra, R. K.; Winge, D. R.; Armitage, I. M. *J. Am. Chem. Soc.* **1991**, *113*, 9354–9358.

and $2.44 \pm 0.03 \text{ \AA}$ for Ag₁₇-MT 1, surprisingly close to each other. The Ag–S bond lengths in Ag(I)–thiolate model compounds with the different coordination geometries of Ag(I) from single-crystal data in Table 4 can be used to infer the Ag(I) coordination numbers in Ag_n-MT complexes. Average Ag–S bond lengths for Ag–thiolate clusters in inorganic compounds are 2.41 \AA for digonal Ag(I) coordination and 2.53 \AA for trigonal Ag(I) coordination, respectively.^{49,60} Therefore, our data reasonably suggest that Ag(I) in both proteins adopts predominantly digonal coordination and clearly preclude the possibility that the Ag(I) coordination geometry changes from trigonal in Ag₁₂-MT 1 to digonal in Ag₁₇-MT 1. This conclusion is further confirmed by the Ag K-edge EXAFS data.⁶¹ The sulfur coordination numbers in these two silver metallothioneins are 1.4 ± 0.3 for Ag₁₂-MT 1 and 1.6 ± 0.5 for Ag₁₇-MT 1. According to the formulas Ag₁₂S₂₀ for Ag₁₂-MT and Ag₁₇S₂₀ for Ag₁₇-MT and sulfur coordination numbers obtained from sulfur K-edge EXAFS measurements, we tentatively suggest that 4 bridging and 16 terminal sulfurs are present in Ag₁₂-MT 1 and that 14 bridging and 6 terminal sulfurs are present in Ag₁₇-MT 1. On the basis of this model, the coordination numbers of sulfur can be calculated to be 1.2 for Ag₁₂-MT 1 (x_t and x_d are 0.8 and 0.2, respectively) and 1.7 for Ag₁₇-MT 1 (x_t and x_d are 0.3 and 0.7, respectively), which are close to the numbers obtained from our sulfur K-edge EXAFS measurements. These results are summarized in Table 2. Since silver(I) in these two proteins has a digonal geometry, the difference of bond lengths between Ag–S_{bridging} and Ag–S_{terminal} is small.⁶² Therefore, the average Ag–S bond distances in these two silver(I)-containing metallothioneins are similar. As the equivalent number of Ag(I) increases from 12 to 17 with more bonds forming, the fraction of bridging sulfurs becomes higher. As a result, the silver–thiolate cluster will tend to form a more twisted-chain structure and change the tertiary structure as a whole, which will be different from the structure in which more terminal sulfurs are involved in Ag₁₂-MT 1. Therefore, the significant changes in CD spectra observed from 12 Ag(I) to 17 Ag(I) may be ascribed to the difference in the three-dimensional structures due to the different fractions of bridging and terminal sulfurs in these two silver(I) proteins. This explanation accounts for the similarity in the CD spectral band energies and signs as Ag(I) is added. Unlike the spectral data recorded during Cu(I) binding where the dramatic changes take place past 12 Cu(I) and the Cu(I)–thiolate cluster unwinds past 15 Cu(I),⁴⁸ the CD data shown in Figure 9 are surprisingly similar for the entire range of Ag(I):MT molar ratios. This

result, established by both low- and high-energy optical methods, suggests that the three-dimensional structures of the metal-binding sites in metallothioneins are strongly influenced by the fraction of bridging sulfur. This analysis is the first to provide direct support for the presence of a clustered Ag–S structure for the Ag₁₇-MT 1 species. These data also suggest that the structures in Ag(I) and Cu(I) metallothioneins are probably quite different.

Conclusion

The structural parameters for [M₄(SPh)₁₀]²⁻ (M = Cd²⁺, Zn²⁺), M₇-MT (M = Cd²⁺, Zn²⁺), M₁₂-MT (M = Cu⁺, Ag⁺), and Ag₁₇-MT have been obtained from analysis of sulfur K-edge EXAFS data. M–S bond distances of $2.52 \pm 0.02 \text{ \AA}$ in Cd₄(SPh)₁₀²⁻ and $2.35 \pm 0.03 \text{ \AA}$ in Zn₄(SPh)₁₀²⁻ are in good agreement with the single-crystal structure data. For Cd₇-MT and Zn₇-MT, the bond lengths are estimated to be 2.54 ± 0.02 and $2.34 \pm 0.03 \text{ \AA}$, respectively, consistent with the results from the metal K-edge EXAFS measurements. Cu(I) has a trigonal coordination in Cu₁₂-MT with Cu–S = $2.25 \pm 0.01 \text{ \AA}$ and a high fraction of bridging sulfurs. With Ag–S bond lengths $2.45 \pm 0.02 \text{ \AA}$ for Ag₁₂-MT and $2.44 \pm 0.03 \text{ \AA}$ for Ag₁₇-MT, Ag(I) in these two proteins has a digonal geometry but a different fraction of bridging and terminal sulfurs. We suggest that more twisted-chain clusters are present in Ag₁₇-MT 1 than in Ag₁₂-MT.

CD spectroscopy is an essential technique for identifying metal-MT species with well-defined tertiary structures. During titration of apo-MT 1 with Ag(I) at low pH and 50 °C, Ag₁₂-MT 1 is characterized by the CD bands at 263 nm (–, very strong) and 314 nm (+, strong), and Ag₁₇-MT 1 is identified by the CD bands at 302 nm (+, very strong) and 370 nm (–, weak). The difference in the CD features of these two silver metallothioneins is attributed to changes in the tertiary structures that arise from changes in the fraction of bridging and terminal sulfurs, rather than from changes in coordination geometry around the Ag(I).

Acknowledgment. We wish to thank, Dr. P. A. W. Dean of UWO for providing us with the Zn(II) and Cd(II) model compounds. We thank Dr. K. R. Bauchspies for providing us with the curve-fitting program, Dr. D.-T. Jiang for helpful discussions, and Dr. T. Tylliszczak for the Ban program used for background subtraction from raw EXAFS data. This project was supported by NSERC Operating and Strategic Grants to M.J.S. and NSERC and NRC Grants to G.M.B. M.J.S. and G.M.B. are members of the Center for Chemical Physics at UWO. We also acknowledge the technical assistance of the staff at the Aladdin Synchrotron Radiation Center and the NSF grant (DMR-9212658) that supports the SRC. This is publication No. 526 of the Photochemistry Unit at UWO.

Supporting Information Available: Figures 5, 6, and 8, showing two-dimensional CD spectra and additional $k\chi(k)$ plots (4 pages). Ordering information is given on any current masthead page.

IC951624M

(60) Dance, I. G.; Fitzpatrick, L. J.; Craig, D. C.; Scudder, M. L. *Inorg. Chem.* **1989**, *28*, 1853–1861.

(61) Gui, Z. Ph.D. Thesis, Department of Chemistry, University of Western Ontario, 1995.

(62) Yamaguchi, H.; Kido, A.; Uechi, T.; Yasukouchi, K. *Bull. Chem. Soc. Jpn.* **1976**, *49*, 1271–1276.

(63) Schuerman, J. A.; Fronczek, F. R.; Selbin, J. *Inorg. Chim. Acta* **1989**, *160*, 43–52.